J Therm Anal Calorim (2012) 108:1101–1110
DOI 10.1007/s10973-011-1987-6

Hydrothermal synthesis, thermal and luminescent investigations of lanthanide(III) coordination polymers based on the 4,4′-oxybis(benzoate) ligand

Renata Łyszczek

ICVMTT2011 Conference Special Chapter

Abstract In this study, new series of lanthanide 4,4′-oxybis(benzoates) of the general formula $Ln_2oba_3 \cdot nH_2O$, where Ln = lanthanides from La(III) to Lu(III), oba = $C_{12}H_8O(COO)_2^{2-}$ and $n = 3$–6, has been prepared under hydrothermal conditions. The compounds were characterized by elemental analysis, infrared spectroscopy, X-ray diffraction patterns measurements and different methods of thermal analysis (TG, DSC, and TG-FTIR). In addition, photoluminescence properties of the selected complexes have been investigated. Crystalline compounds are isostructural in the whole series. Both carboxylate groups are deprotonated and engaged in the coordination of Ln(III) ions. Heating of the complexes leads to the dehydration and next decomposition processes. Although of the same structure, the removal of water molecules proceeds in different ways. In the nitrogen atmosphere, they decompose releasing water, carbon oxides and phenol molecules. The complexes of Eu(III), Tb(III) and Dy(III) exhibit photoluminescence in the visible range, whereas the compounds of Nd(III) and Yb(III) in the near-infrared region upon excitation by UV light.

Keywords Coordination polymers · Lanthanides, 4,4′-oxybis(benzoic) acid · TG-DSC, TG-FTIR · Photoluminescence

Electronic supplementary material The online version of this article (doi:10.1007/s10973-011-1987-6) contains supplementary material, which is available to authorized users.

R. Łyszczek (✉)
Department of General and Coordination Chemistry, Faculty of Chemistry, Maria Curie-Skłodowska University, M.C. Skłodowskiej Sq. 2, 20-031 Lublin, Poland
e-mail: renata.lyszczek@poczta.umcs.lublin.pl

Introduction

The coordination polymers and metal–organic frameworks have received extensive research attention as promising hybrid materials owing to their extraordinary properties such as multidimensional structure, high surface area and sorption of small molecules [1–6]. They are generally synthesized by self-assembly of metal ions as nodes and organic ligands as connectors. Topology of coordination polymers is influenced by many factors, such as geometric preferences of metal ions, geometry of the organic linkers and synthetic conditions (solvent, pH, temperature) [7–9]. The geometry of transition metals can dictate the mode of coordination, whereas the control over the topology of lanthanide coordination polymers is more difficult due to the large and variable coordination numbers of Ln(III) ions. However, many lanthanide coordination polymers or lanthanide–organic frameworks have been investigated because of their unusual architectures and superior functional properties, such as high surface area and ability for gases sorption [10–15], which make them particularly attractive in applications. In addition, magnetic [16–18] and catalytic [19] properties of lanthanide coordination polymers are useful in the discovery of new functional hybrid materials. The lanthanide ions offer an advantage over other metals in the development of luminescent materials. They show sharp intra f–f emissions bands in the visible or near-infrared spectral regions when electronic transitions occur in which make lanthanide MOFs potentially applicable for lighting, optical storage and sensors [20–22].

Polycarboxylate ligands are among the most important and widely employed bridging linkers for the construction of the coordination polymers because these anions can act as bridging ligands with various coordination modes and

they exhibit high affinity for Ln(III) ions. Multifunctional O-donor ligands, such as derivatives of benzoic acid with the carboxylate groups in positions: 1,4-; 1,3- or 1,3,5-, have been widely explored in the preparation of lanthanide–organic frameworks, MOFs [12, 13, 18, 23, 24]. Recently, longer O-donor ligands, such as naphthalene-2,6-dicarboxylate [25, 26], biphenylethene-4,4′-dicarboxylate [27], biphenyl-3,4,5′-tricarboxylate [17] or 4,4′-oxybis(benzoate) [28–32], have been employed as linkers in the multi-dimensional lanthanide coordination polymers.

In this article, this author presents a new series of lanthanide complexes with 4,4′-oxybis(benzoic) acid obtained under hydrothermal conditions. The thermogravimetric (TG), differential scanning calorimetry (DSC) methods in air and TG-FTIR coupled technique in nitrogen were used to study the decomposition pathway of the investigated compounds. In addition, photoluminescent properties of Eu(III), Nd(III), Tb(III), Dy(III) and Yb(III) complexes were studied. 4,4′-oxybis(benzoic) acid was chosen for the synthesis of the lanthanide complexes because its flexible and multifunctional coordination sites may generate multidimensional polymeric structures [28–32].

This study is continuation of this author's research concerning thermal and spectroscopic investigations of lanthanide complexes with polycarboxylic acids [33–37].

Experimental

4,4′-oxybis(benzoic) acid (99%), cerium(III) nitrate(V) hexahydrate (99.99%) and lanthanide oxides (99.9%) were purchased from Aldrich without further purification. Lanthanide chlorides were prepared by dissolving 1 mmol of lanthanide oxide Ln_2O_3 (0.33 mmol of Pr_6O_{11} and 0.5 mmol of Tb_4O_7) in hydrochloric acid and evaporated.

Sodium salt of 4,4′-oxybis(benzoic) acid was prepared by the addition of two equivalents of sodium hydroxide to a suspension of 4,4′-oxybis(benzoic) acid in deionized water. 10 mL of sodium salt (2 mmol, pH = 6.3) was mixed with the aqueous solution of lanthanide(III) chloride [or cerium(III) nitrate(V)] (15 mL, 2 mmol, pH = 4.5). The obtained precipitation was heated in the Teflon-lined autoclave under autogeneous pressure at 160 °C for 5 days, followed by slow cooling to room temperature.

The contents of carbon and hydrogen in the compounds were determined by the elemental analysis using a Perkin-Elmer CHN 2400 elemental analyser (Table S1). The rare earth elements were determined by ignition of the complexes to Ln_2O_3, CeO_2, Pr_6O_{11}, or Tb_4O_7 oxides. The contents of water were established from the TG curves and elemental analysis.

The IR spectra of the free acid and the prepared complexes were recorded over the range 4,000–400 cm^{-1} in KBr discs using a Specord M80 Carl Zeiss Jena spectrophotometer.

The X-ray powder diffractions of the studied compounds were recorded on a HZG 4 diffractometer, using Ni-filtered CuKα radiations. Measurements were taken over the range of 2θ = 5–50° with resolution of 0.05°.

Thermal analyses of the prepared complexes were carried out by the thermogravimetric (TG) and differential scanning calorimetry (DSC) methods using the SETSYS 16/18 analyser (Setaram). The samples (about 5–9 mg) were heated in ceramic crucibles up to 850 °C at a heating rate of 10 °C min^{-1} in dynamic air atmosphere (v = 0.75 dm^3 h^{-1}).

The TG-FTIR measurements have been performed using the Q5000 TA apparatus coupled with Nicolet 670 spectrophotometer. The samples of about 6–10 mg were heated up to 1,000 °C in 100 µL open ceramic crucibles at a heating rate of 20 °C min^{-1} in flowing nitrogen atmosphere (25 mL min^{-1}).

The photoluminescent spectra of the Nd(III), Eu(III), Tb(III), Er(III) and Dy(III) complexes were recorded at room temperature using a Photon Technology International fluorescence spectrophotometer.

Results and discussion

A new series of lanthanide 4,4′-oxybis(benzoates) of the general formula $Ln_2oba_3{\cdot}nH_2O$ (where Ln = lanthanides from La(III) to Lu(III), oba = $C_{12}H_8O(COO)_2^{2-}$ and n = 3 for Ce; four for Pr and Er; five for Eu–Ho, Tm and Lu; 5.5 for La and Sm; and six for Nd and Yb) have been prepared under hydrothermal conditions in the reaction of lanthanide(III) chloride with sodium salt of 4,4′-oxybis(benzoic) acid. Nitrate was used to prepare cerium complex. The results from elemental analysis are given in supplementary material (Table S1). The compounds are hardly soluble in water and common organic solvents (ethanol, methanol, benzene, dimethylformamide, and tetrahydrofurane). The X-ray diffraction pattern analysis reveals that all compounds are crystalline as seen in Fig. 1. Their peak positions are in good agreement with each other, and the most intense bands appear at a very similar value of 2θ angle (5.7; 6.3, 9.4, 11.4, 12.6, 17.1, 18.9 25.3, 31.75, 38.35 and 45) that can be indicative for the similar structure of the whole series of complexes [38].

Infrared spectroscopy analysis

The IR spectra of the investigated compounds allow insights into the chemical compositions of lanthanide 4,4′-oxybis(benzoates). The most characteristic bands and their assignments are shown in Table 1. The band positions are

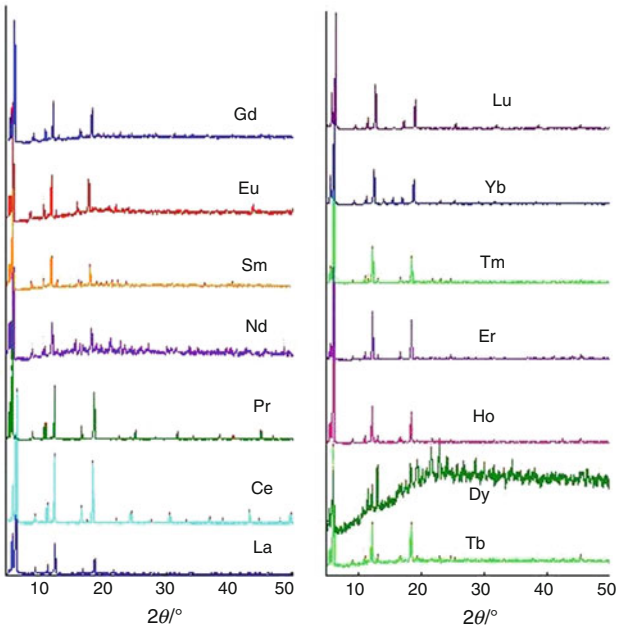

Fig. 1 X-ray diffraction patterns of lanthanide 4,4′-oxybis(benzoates)

almost the same in their infrared spectra, indicating that all the complexes are of a similar structure. They show characteristic bands for the asymmetric [ν_{as}(COO)]- and symmetric [ν_s(COO)]-stretching vibrations of the carboxylate groups in the regions 1,544–1,512 cm^{-1} and 1,432–1,405 cm^{-1}, respectively. These new bands prove that lanthanide ions in the obtained compounds have been coordinated with 4,4′-oxybis(benzoate) ligand successfully [39]. The absence of the absorption bands of the nonionized carboxylic groups of free acid at 1,690; 1,680 cm^{-1} [ν(CO)]; 1,260 cm^{-1} [ν(COH)] and 936 cm^{-1} [δ(OH)] confirmed the complete deprotonation of acid (Fig. 2). It is concluded that the compounds are of polymeric structures as a result of preferences of oba^{2-} ligand for bridging of metal ions [28–32]. All spectra show broad bands in the range 3,700–2,830 cm^{-1}, which confirms the presence of hydrogen-bonded water molecules in the structures. These bands were assigned to the stretching vibrations of hydroxyl groups ν(OH) of water molecules. Stretching vibrations $\nu(C_{Ar}O)$ from the aryl ether group C_{Ar}–O–C_{Ar} were found in the region 1,264–1,256 cm^{-1}. An intense band in the range 1,624–1,596 cm^{-1} and weaker bands at 1,560; 1,544 and 1,504 cm^{-1} common to all compounds were assigned to the stretching vibrational modes of aromatic rings $\nu(C_{Ar}C_{Ar})$. The bands at about 1,164; 1,096; and 1,012 cm^{-1} were assigned to the in-plane bending vibrations of the ring. The remaining vibrational bands present in the region 1,000–600 cm^{-1} are characteristic of 1,4-disubstituted benzene rings and derived from the out-of-plane bending vibrations of $C_{Ar}H$ bonds and out-of-plane ring $C_{Ar}C_{Ar}$ bend [40].

TG-DSC analyses in air

The thermal stability and behaviour of the investigated complexes during heating were investigated by means of TG analysis, DSC in air and TG-FTIR coupled techniques in nitrogen. All investigated compounds are stable at room temperature. The thermal decomposition of lanthanide 4,4′-oxybis(benzoates) in air proceeds in two main stages including dehydration process and degradation of anhydrous species. Heating of the compounds resulted in the release of water molecules in different pathways (Figs. 3, 4, 5, 6), although that the obtained complexes are isostructural. They generally start to lose water molecules in the

Table 1 Frequencies of characteristic absorption bands in the IR spectra of lanthanide 4,4′-oxybis(benzoates), (oba = $C_{12}H_8O(COO)_2^{2-}$)

Compound	ν(OH)	ν_{asym}(COO)	ν_{sym}(COO)	$\nu(C_{Ar}C_{Ar})$	$\nu(C_{Ar}O)$
$La_2oba_3{\cdot}5.5H_2O$	3,670–3,070	1,524; 1,512	1,412; 1,400	1,600; 1,560	1,260
$Ce_2oba_3{\cdot}3H_2O$	3,650–3,000	1,524	1,408	1,596; 1,504	1,260
$Pr_2oba_3{\cdot}4H_2O$	3,660–3,000	1,524	1,408	1,596; 1,504	1,264
$Nd_2oba_3{\cdot}6H_2O$	3,650–3,080	1,528; 1,512	1,412	1,600; 1,560; 1,504	1,264
$Sm_2oba_3{\cdot}5.5H_2O$	3,670–3,080	1,524	1,412	1,596; 1,544	1,260
$Eu_2oba_3{\cdot}5H_2O$	3,670–3,000	1,524	1,408	1,596; 1,504	1,260
$Gd_2oba_3{\cdot}5H_2O$	3,680–3,080	1,532	1,416	1,596; 1,500	1,260
$Tb_2oba_3{\cdot}5H_2O$	3,690–3,050	1,532	1,416	1,596; 1,504	1,260
$Dy_2oba_3{\cdot}5H_2O$	3,700–3,000	1,528	1,416	1,596; 1,504	1,260
$Ho_2oba_3{\cdot}5H_2O$	3,700–3,000	1,536	1,416	1,596; 1,504	1,260
$Er_2oba_3{\cdot}4H_2O$	3,650–3,100	1,533	1,406	1,596; 1,504	1,260
$Tm_2oba_3{\cdot}5H_2O$	3,700–3,080	1,536	1,416	1,596; 1,504	1,260
$Yb_2oba_3{\cdot}6H_2O$	3,700–2,950	1,544	1,432	1,620; 1,596	1,260
$Lu_2oba_3{\cdot}5H_2O$	3,680–2,830	1,540	1,420	1,624; 1,596	1,256

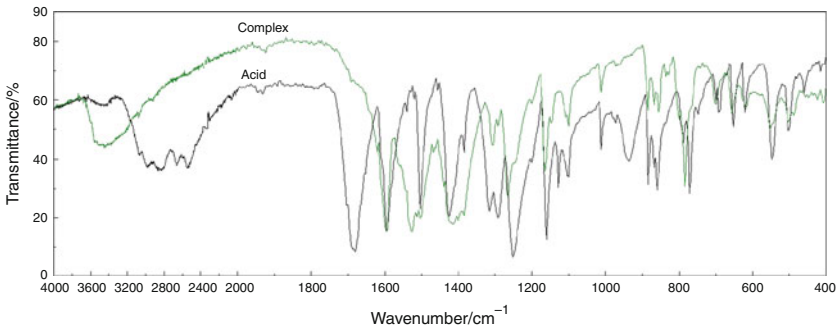

Fig. 2 Infrared spectra of free 4,4′-oxybis(benzoic) acid and $Nd_2oba_3{\cdot}6H_2O$ complex

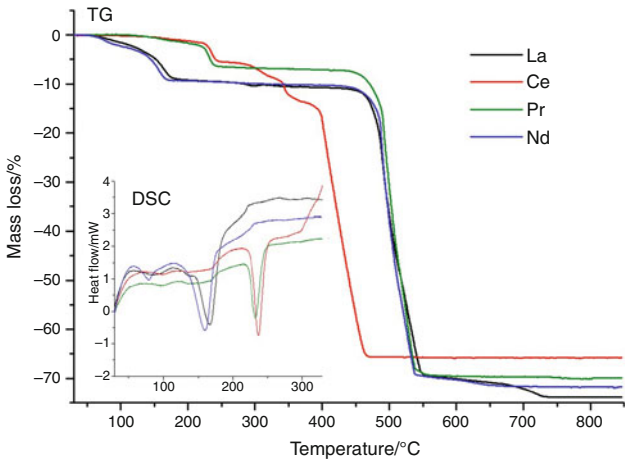

Fig. 3 TG curves of thermal decomposition (air) of complexes: $La_2oba_3{\cdot}5.5H_2O$, $Ce_2oba_3{\cdot}3H_2O$, $Pr_2oba_3{\cdot}4H_2O$ and $Nd_2oba_3{\cdot}6H_2O$. The *inset* shows DSC curves recorded in the temperature of dehydration

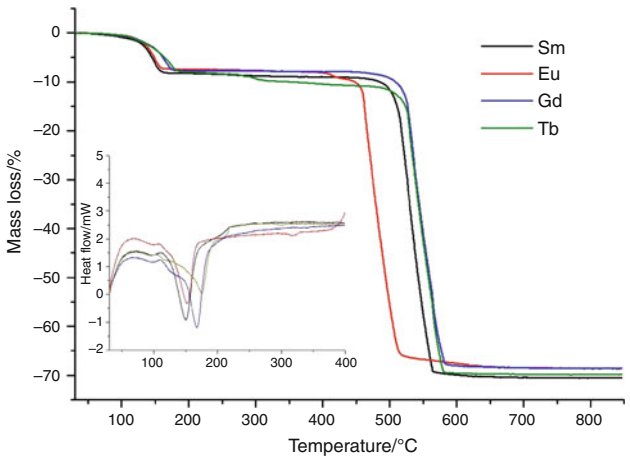

Fig. 4 TG curves of thermal decomposition (air) of complexes: $Sm_2oba_3{\cdot}5.5H_2O$, $Eu_2oba_3{\cdot}5H_2O$, $Gd_2oba_3{\cdot}5H_2O$ and $Tb_2oba_3{\cdot}5H_2O$. The *inset* shows DSC curves recorded in the temperature of dehydration

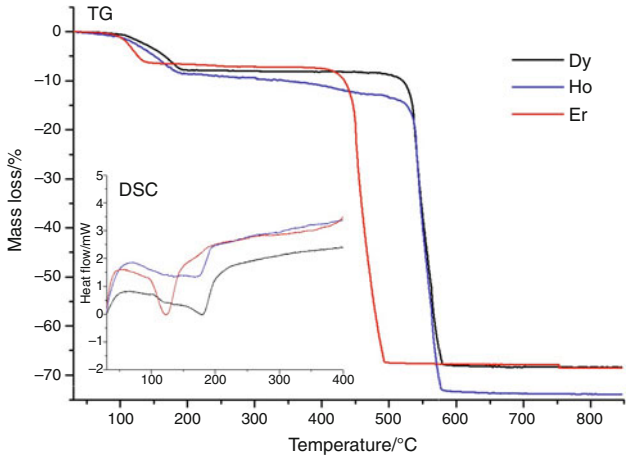

Fig. 5 TG curves of thermal decomposition (air) of complexes: $Dy_2oba_3{\cdot}5H_2O$, $Ho_2oba_3{\cdot}5H_2O$ and $Er_2oba_3{\cdot}4H_2O$. The *inset* shows DSC curves recorded in the temperature of dehydration

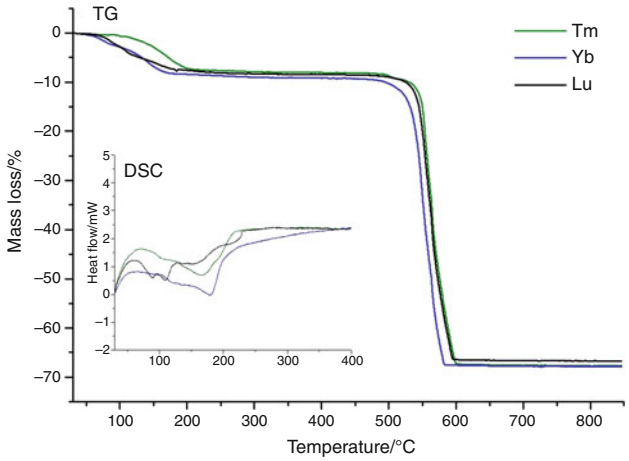

Fig. 6 TG curves of thermal decomposition (air) of complexes: $Tm_2oba_3{\cdot}5H_2O$, $Yb_2oba_3{\cdot}6H_2O$ and $Lu_2oba_3{\cdot}5H_2O$. The *inset* shows DSC curves recorded in the temperature of dehydration

range 40–75 °C but Ce and Pr complexes exhibit greater thermal stability (up to 120 and 110 °C, respectively). Also evolution of water molecules occurs in various temperature ranges as can be seen from Table 2. The TG profiles of Sm, Eu, Gd, Tb, Dy, Er, Tm and Ho complexes indicate that water molecules are released in one step. Although, only one obvious weight loss is observed, the shapes of peaks on the DSC curves indicate that water molecules are liberated in the overlapping stages (Table 2; Figs. 4, 5, 6). For the

Table 2 Thermogravimetric data obtained during heating of lanthanide(III) 4,4′-oxybis(benzoates) in air atmosphere

Compound	ΔT_1/°C	Evolved molecules	Mass loss/%		T_2/°C	ΔH/kJ mol^{-1}	ΔT_3	T_4/°C	Mass loss/%	
			Cal.	Found					Cal.	Found
$La_2oba_3{\cdot}5.5H_2O$	50–110	$1.5H_2O$	2.35	2.20	168	116	170–430	730	71.56	73.60
	110–170	$4H_2O$	6.29	6.51						
$Ce_2oba_3{\cdot}3H_2O$	120–225	H_2O	1.60	1.80	235	117	245–270	470	68.72	65.59
	225–240	$2H_2O$	3.29	3.21						
$Pr_2oba_3{\cdot}4H_2O$	110–220	$1.5H_2O$	2.41	2.50	232	110	240–410	570	69.66	69.50
	220–240	$2.5H_2O$	4.01	4.40						
$Nd_2oba_3{\cdot}6H_2O$	50–110	$2H_2O$	3.09	9.00	160	180	170–410	660	71.12	71.69
	110–170	$4H_2O$	6.18							
$Sm_2oba_3{\cdot}5.5H_2O$	60–165	$5.5H_2O$	8.47	7.95	150	220	165–440	670	70.15	70.40
$Eu_2oba_3{\cdot}5H_2O$	50–165	$5H_2O$	7.74	7.62	157	213	165–420	560	69.73	70.66
$Gd_2oba_3{\cdot}5H_2O$	60–180	$5H_2O$	7.67	7.52	167	233	180–450	590	69.10	67.93
$Tb_2oba_3{\cdot}5H_2O$	55–188	$5H_2O$	7.65	7.86	175	186	190–450*	585	68.52	69.13
$Dy_2oba_3{\cdot}5H_2O$	55–190	$5H_2O$	7.60	7.64	180	215	190–480	590	68.57	68.04
$Ho_2oba_3{\cdot}5H_2O$	75–185	$5H_2O$	7.57	7.71	179	248	190–480**	580	68.2	73.40
$Er_2oba_3{\cdot}4H_2O$	70–162	$4H_2O$	6.12	6.22	147	126	160–420	590	67.49	67.58
$Tm_2oba_3{\cdot}5H_2O$	50–200	$5H_2O$	7.50	6.90	169	204	200–460	600	67.75	67.67
$Yb_2oba_3{\cdot}6H_2O$	40–85	$2H_2O$	2.94	2.57	170	137	170–460	600	67.53	67.88
	85–170	$4H_2O$	5.88	5.49						
$Lu_2oba_3{\cdot}5H_2O$	45–100	H_2O	1.49	1.20	90	–	270–460	600	67.32	66.34
	100–120	H_2O	1.49	1.20	108					
	120–270	$3H_2O$	3.63	5.40	159					

ΔT_1—temperature range of dehydration; T_2—temperature of endothermic peaks (*top*); ΔH—value of enthalpy of dehydration reaction measured for higher temperature; ΔT_3—temperature range of stability of Ln_2oba_3; T_4—temperature of lanthanide oxide formation; *—temperature range of mass loss of 2.85%; **—temperature range of mass loss of 4.47%

remaining compounds, two (La, Ce, Pr, Nd and Yb) or three (Lu) better-separated stages of dehydration can be distinguished (Figs. 3, 6; Table 2). For Ce(III) and Pr(III) compounds, departure of water molecules occurs in an entirely different way compared with the remaining complexes. At first, continuous weight loss is observed in a relatively broad temperature range (110–225 °C) along with evolution of 1 or 1.5 water molecules. Next, a sharp mass loss occurs in a narrow temperature range (220–240 °C) which is accompanied by a sharp endothermic effect with the peak top at 235 °C (for Ce) and 232 °C (for Pr). For the La, Nd, and Yb complexes, the two-step dehydration process corresponds to release of 1.5 or 2 water molecules in the first step and 4 molecules in the next one, respectively. Removal of water molecules in the Lu compound takes place in a more complicated way. Based only on the TG curve, it is difficult to separate dehydration stages. However, profile of DSC curve shows three subsequent endothermic effects at 90, 108 and 159 °C which allows us to postulate stepwise dehydration (Fig. 6).

The highest temperature of the endothermic effect assigned to the departure of water molecules in the group of light lanthanide compounds (from La to Gd) is observed for Ce and Pr compounds. In the remaining complexes (La, Nd, Sm and Eu), endothermic DSC effects are observed at 168, 160, 150 and 157 °C, respectively. Considering the dehydration process of heavy lanthanides (from Tb to Lu), it is concluded that the lowest temperature of endothermic effects connected with release of water molecules are observed for the Lu and Er compounds (147 °C). For the Dy, Ho, Tm and Yb compounds, the endothermic effects at 180, 179, 169 and 170 °C, respectively were recorded. The dehydration enthalpies found for lanthanide 4,4′-oxybis(benzoates) were in the range of 110–248 kJ mol^{-1}.

We can assume that water molecules evolved at a lower temperature are weakly bonded in the structure. They probably occupy positions in the cavities being hydrogen bonded with the metal–organic framework. On the contrary, water molecules depart at a higher temperature being more strongly bonded in the investigated compounds, which can be due to their different arrangements in the structure or even coordination with metal ions.

Departure of the water molecules from the structures leads to the formation of anhydrous compounds of the formula Ln_2oba_3, which are stable in various temperature ranges. Only Ce_2oba_3 is unstable, and it decomposes

directly after the dehydration process without showing any plateau. The remaining light lanthanide complexes are thermally stable up to about 410–450 °C, whereas the heavy lanthanide compounds demonstrate insignificantly higher stability at 460–480 °C (except Er complex—420 °C). For the Tb(III) and Ho(III) complexes in the ranges of 190–450 and 190–480 °C, continuous mass losses of 2.85 and 4.47%, respectively, are recorded. These phenomena can be attributed to the incomplete removal of solvent molecules from the structure or partial degradation of anhydrous compounds. In addition, for the Ho complex, small endothermic effect at 450 °C is observed.

Upon further heating, distinct weight losses observed on the TG correspond to the degradation of Ln_2oba_3 compounds and burning of organic ligands. Lanthanide oxides (CeO_2, Pr_6O_{11}, Tb_4O_7 and Ln_2O_3 for the remaining complexes) are the final products of complexes decomposition in air [41]. They are formed in the temperature range of 470–730 °C.

TG-FTIR analysis in nitrogen

The simultaneous TG analysis in nitrogen coupled with the FTIR spectrophotometric analysis allows determining the pathway of complexes decomposition in air-free atmosphere (Table 3) and identification of their volatile products of degradation. Based on the obtained results, it is postulated that thermal stability of the complexes in the nitrogen atmosphere slightly increased. The dehydration process in the group of light lanthanide compounds occurs almost in the same way as in air atmosphere. Only for the Nd complex, departure of water molecules takes place in a different way. The TG analysis of heavy lanthanide compounds confirmed multi-step dehydration of the Lu complex. We note that the TG curves of Tb and Er complexes show two weight losses in the temperature range of dehydration, whereas in air, only one stage was observed. It is also established that the dehydrated forms of complexes (Ln_2oba_3) are more thermally stable (Table 3, supplementary materials Figures A1 and A2) in nitrogen compared with air atmosphere (Table 2). Among light lanthanide compounds, Ce and Eu compounds start to decompose at the lower temperatures, i.e., 310 and 450 °C, respectively. The compounds of heavy lanthanides begin to decompose at above 500 °C. Further heating, resulted in the formation of lanthanide oxides in the case of some complexes (La, Sm-Dy, Er-Lu), whereas the remaining compounds (Ce, Nd, Pr and Ho) degradate to undefined species (probably mixture of lanthanide oxides and carbon).

The TG-FTIR analysis was performed to detect of the volatile products of thermal decomposition of the

Table 3 Thermogravimetric data obtained during heating of lanthanide(III) 4,4′-oxybis(benzoates) in nitrogen atmosphere

Compound	ΔT_1/°C	Mass loss/% (found)	ΔT_2/°C	T_3/°C (final solid product)	Mass loss/% (found)
$La_2oba_3 \cdot 5.5H_2O$	65–164	8.22	164–476	857 (La_2O_3)	72.64
$Ce_2oba_3 \cdot 3H_2O$	108–183	1.67	–	1,000 (C + CeO_2)	64.80
	83–248	3.60			
	248–310	6.70			
$Pr_2oba_3 \cdot 4H_2O$	120–258	6.40	258–527	1,000 (C + Pr_6O_{11})	51.37
$Nd_2oba_3 \cdot 6H_2O$	92–166	9.10	311–510	1,000 (C + Nd_2O_3)	50.50
$Sm_2oba_3 \cdot 5.5H_2O$	100–162	7.18	166–515	930 (Sm_2O_3)	67.73
$Eu_2oba_3 \cdot 5H_2O$	56–175	8.00	174–450	550 (Eu_2O_3)	69.60
$Gd_2oba_3 \cdot 5H_2O$	55–178	8.00	178–460	653 (Gd_2O_3)	70.00
$Tb_2oba_3 \cdot 5H_2O$	67–193	7.65	290–504	795 (Tb_4O_7)	71.50
	193–289	2.59			
$Dy_2oba_3 \cdot 5H_2O$	70–215	7.50	215–515	810 (Dy_2O_3)	69.50
$Ho_2oba_3 \cdot 5H_2O$	66–210	7.70	210–525	1,000 (C + Ho_2O)	54.04
$Er_2oba_3 \cdot 4H_2O$	100–212	7.20	307–508	648 (Er_2O_3)	69.03
	212–307	2.52			
$Tm_2oba_3 \cdot 5H_2O$	100–210	6.85	210–510	590 (Tm_2O_3)	67.21
$Yb_2oba_3 \cdot 6H_2O$	60–180	6.00	180–523	930 (Yb_2O_3)	67.19
$Lu_2oba_3 \cdot 5H_2O$	60–90	3.07	247–512	1,000 (Lu_2O_3)	64.50
	90–116	2.30			
	116–247	4.11			

ΔT_1—temperature range of dehydration; ΔT_2—temperature range of stability of Ln_2oba_3; ΔT_3—temperature of final products formation

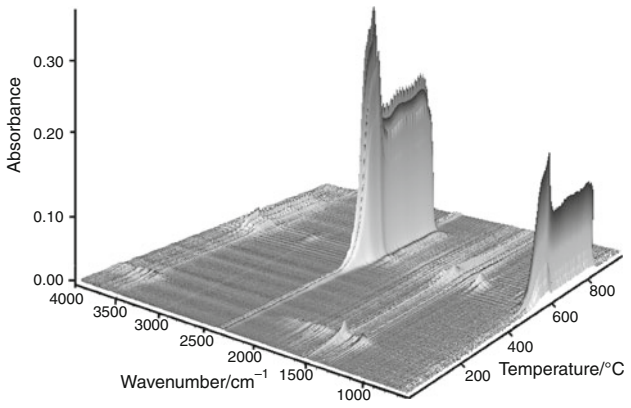

Fig. 7 Stacked plot of FTIR spectra of the evolved gases for $La_2oba_3{\cdot}5.5H_2O$ (nitrogen)

investigated compounds during heating in nitrogen. The $La_2obb_3{\cdot}5.5H_2O$ compound was taken as a representative of a series of 4,4′-oxybis(benzoates). The Gram–Schmidt curve (supplementary material) clearly shows a weak peak in the temperature range 80–180 °C and very strong peak with the maximum at 560 °C. The TG-FTIR spectra recorded up to about 250 °C show characteristic bands in the wavenumber ranges 4,000–3,500 and 1,800–1,300 cm^{-1} assigned to the stretching and deformation vibrations of hydroxyl groups ν(O–H) from water molecules (Fig. 7). The formation of stable intermediate products of dehydration (Ln_2oba_3) is confirmed by the almost linear Gram–Schmidt plot and a lack of absorption bands on the FTIR spectra. Above 400 °C, a stacked plot of FTIR spectra shows a characteristic doublet band with maxima at 2,357 and 2,344 cm^{-1} and those in the range 750–600 cm^{-1}, because of stretching and deformation vibrations of carbon dioxide molecules [42]. This product is formed probably as a consequence of disruption of lanthanide–organic ligand bonds. At a higher temperature (about 520 °C), besides CO_2 bands, a diagnostic double-band at 2,181 and 2,107 cm^{-1} due to the presence of carbon oxide is observed. Simultaneously, phenol molecules are evolved as confirmed by the bands at: 3,058 cm^{-1} from the stretching vibrations of (C_{Ar}–H): 1,593 and 1,488 cm^{-1} due to the stretching vibrations of the aromatic ring ($C_{Ar}C_{Ar}$): 1,339 cm^{-1} from in-plane bending mode of (OH): 1,242 cm^{-1} from the stretching vibrations of ($C_{Ar}O$): 1,184; 1,057; 1,023 cm^{-1}; and 863 cm^{-1} in-plane and out-of-plane bending vibrations of (CH) groups, respectively [40]. The most intense evolution of volatile products (carbon oxides and phenol) was observed at 590 °C (Fig. 8). At higher temperatures, up to about 880 °C, only carbon oxides were detected as the products of the complex decomposition.

Photoluminescent properties

Taking into account the excellent luminescent properties of lanthanide ions within the carboxylate ligands, the luminescent properties of the selected compounds were investigated in the solid state at room temperature. The $Eu_2oba_3{\cdot}5H_2O$, $Tb_2oba_3{\cdot}5H_2O$ and $Dy_2oba_3{\cdot}5H_2O$ complexes were chosen to investigate their photoluminescent spectra in the visible spectral region [17, 43]. The emission spectra of $Nd_2oba_3{\cdot}6H_2O$ and $Yb_2oba_3{\cdot}6H_2O$ compounds were investigated in the NIR region. The emission spectra of all compounds at the excited wavelength of 350 nm display the characteristic f–f emissions of Eu(III), Tb(III), Dy(III), Nd(III) and Yb(III) ions.

For the $Eu_2oba_3{\cdot}5H_2O$ complex, four characteristic bands are shown in Fig. 9. The emissions at 591, 616, 654 and 699 nm were assigned to the transitions from the excited $^5D_0$ level to the multiplet ^7F_J ($J = 1, 2, 3, 4$) levels of the Eu(III) ions, respectively. The most intense transition is $^5D_0 \rightarrow {}^7F_2$, which implies red emission of the Eu complex. The intensity of the $^5D_0 \rightarrow {}^7F_2$ transition of electric dipole character is stronger than that of the $^5D_0 \rightarrow {}^7F_1$ transition of magnetic dipole nature, and it

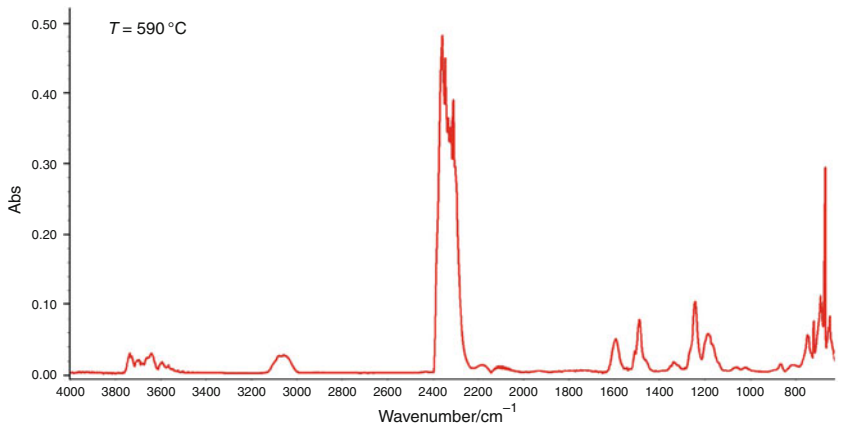

Fig. 8 FTIR spectrum of volatile products of thermal decomposition of $La_2oba_3{\cdot}5.5H_2O$ recorded at 480 °C

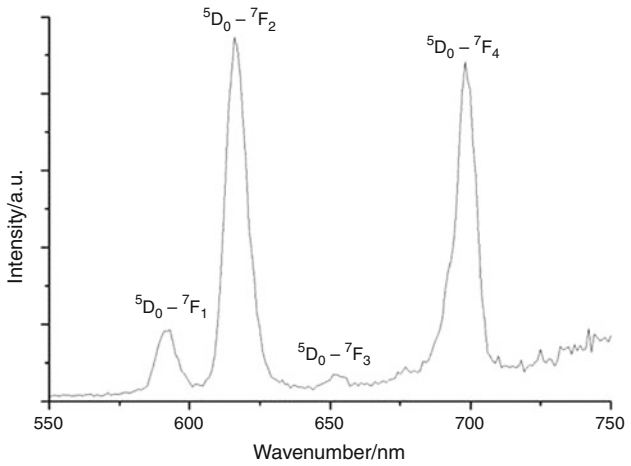

Fig. 9 Photoluminescent spectrum of $Eu_2oba_3{\cdot}5H_2O$

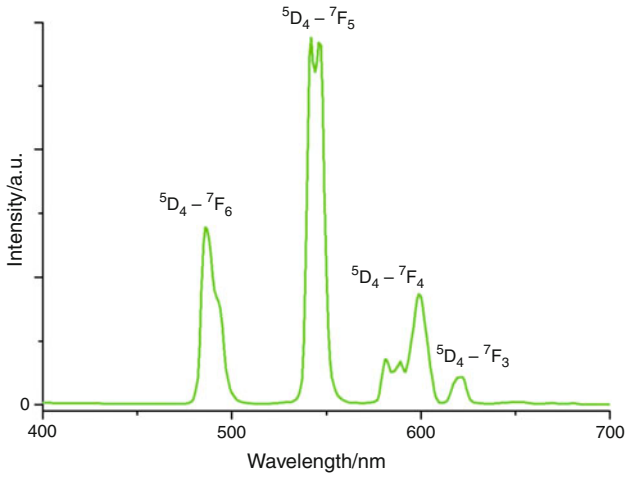

Fig. 10 Photoluminescent spectrum of $Tb_2oba_3{\cdot}5H_2O$

indicates asymmetric coordination environment of europium(III) ions [20, 22, 43].

The emission spectrum of the terbium complex, $Tb_2oba_3{\cdot}5H_2O$ (Fig. 10), exhibits the characteristic transitions of $^5D_4 \rightarrow {}^7F_J$ ($J = 3$–6) of the Tb(III) ion. The band at 488 nm and doublet at 544 and 550 nm correspond to the $^5D_4 \rightarrow {}^7F_6$ and $^5D_4 \rightarrow {}^7F_5$ transitions, respectively. These emissions give an intense green luminescence. The weaker emission bands at 580 and 618 nm originate from the $^5D_4 \rightarrow {}^7F_4$ and $^5D_4 \rightarrow {}^7F_3$ transition, respectively.

The characteristic yellow emissions of Dy(III) ions in the $Dy_2oba_3{\cdot}5H_2O$ complex are shown in Fig. 11. Two peaks at 475 and 570 nm in the visible light region were assigned to the $^4F_{9/2} \rightarrow {}^6H_{15/2}$ and $^4F_{9/2} \rightarrow {}^6H_{13/2}$ transition, respectively.

The emission spectrum of the $Nd_2oba_3{\cdot}6H_2O$ complex shows two characteristic f–f transition bands at 1,052 and

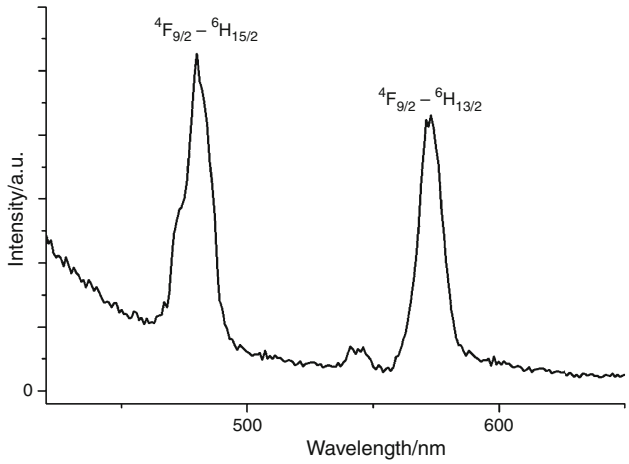

Fig. 11 Photoluminescent spectrum of $Dy_2oba_3{\cdot}5H_2O$

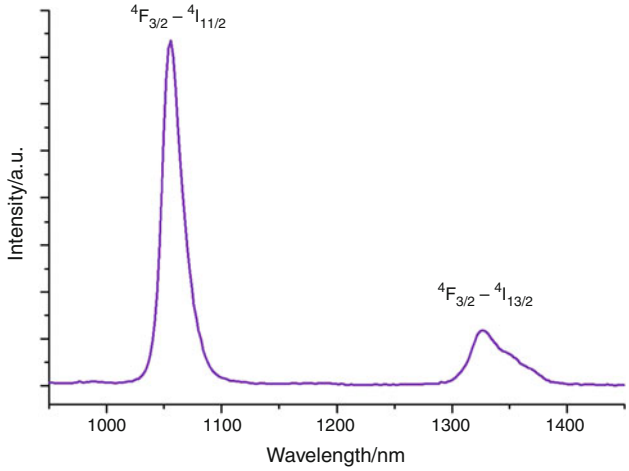

Fig. 12 Photoluminescent spectrum of $Nd_2oba_3{\cdot}6H_2O$

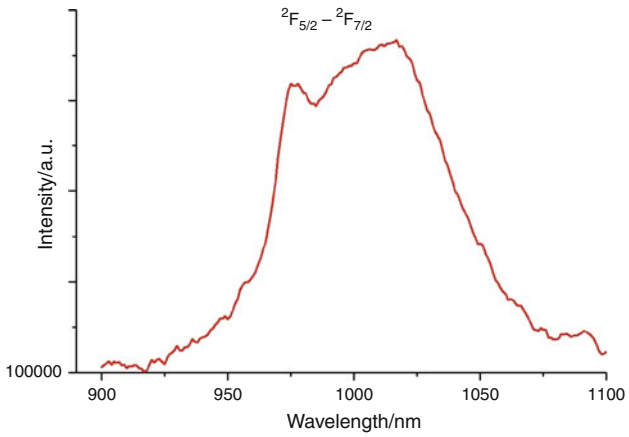

Fig. 13 Photoluminescent spectrum of $Yb_2oba_3{\cdot}6H_2O$

1,384 nm (Fig. 12). These bands were attributed to the $^4F_{3/2} \rightarrow {}^4I_{11/2}$ and $^4F_{3/2} \rightarrow {}^4I_{13/2}$ transitions of Nd(III) ion, respectively.

The NIR spectrum of $Yb_2obb_3{\cdot}6H_2O$ complex displays a broad peak upon excitation at 350 nm (Fig. 13). The split band with the submaxima at 972, 997 and 1,018 nm was assigned to the $^2F_{5/2} \rightarrow {}^2F_{7/2}$ transition [17, 20–22, 43].

It is well known that water molecules quench the emissions. Although all compounds have been obtained in the form of hydrates, the characteristic emissions of Ln(III) are still strong. This could be ascribed to high efficiency of energy transfer from ligand to lanthanide ions.

Conclusions

In this article, a new series of lanthanide 4,4′-oxybis(benzoates) coordination polymers has been characterized. The whole series of complexes (from La to Lu) is of the same crystal structure as can be deduced from their XRD patterns. The oba^{2-} ligand coordinates Ln(III) ions through both deprotonated carboxylate groups. Compounds are thermally stable at room temperature but further heating causes departure of water molecules in different ways. Water molecules were detected in the FTIR spectra of gaseous products of complexes decomposition. The dehydration process yields formation of stable intermediate products that are further degradated with evolution of carbon oxides and phenol molecules (nitrogen). The atmosphere of heating slightly influences on the pathway of compounds decomposition, especially the increase in the thermal stability of both hydrated and anhydrous compounds. The complexes of Eu, Tb and Dy show red, green and yellow light emission upon excitation by UV light. The compounds of Nd and Yb emit light in the near-infrared range of spectrum.

References

1. Navarro JAR, Barea E, Sales JM, Masciocchi N, Galli S, Sironi A, Ania CA, Parra JB. H_2, N_2, CO, and CO_2 sorption properties of a series of robust sodalite-type microporous coordination polymers. Inorg Chem. 2006;45:2397–9.
2. Janiak C. Engineering coordination polymers towards applications. Dalton Trans. 2003;14:2781–804.
3. Furukawa H, Miller MA, Yaghi OM. Independent verification of the saturation hydrogen uptake in MOF-177 and establishment of a benchmark for hydrogen adsorption in metal-organic frameworks. J Mater Chem. 2007;17:3197–204.
4. Meek ST, Greathouse JA, Allendorf MD. Metal-organic frameworks: a rapidly growing class of versatile nanoporous materials. Adv Mater. 2011;23:249–67.
5. Li JR, Kuppler RJ, Zhou HC. Selective gas adsorption in metal-organic frameworks. Chem Soc Rev. 2009;38:1477–504.
6. Li H, Eddaoudi M, O'Keeffe M, Yaghi OM. Design and synthesis of an exceptionally stable and highly porous metal-organic framework. Nature. 1999;402:276–9.
7. Shimizu GKH. Assembly of metal ions and ligands with adaptable coordinative tendencies as a route to functional metal-organic solids. J Solid State Chem. 2005;178:2519–26.
8. Pan L, Huang X, Li J, Wu Y, Zheng N. Novel single- and double-layer and three-dimensional structures of rare-earth metal coordination polymers: the effect of lanthanide contraction and acidity control in crystal structure formation. Angew Chem Int Ed. 2000;39:527–30.
9. Khan NA, Jun JW, Jhung SH. Effect of water concentration and acidity on the synthesis of porous chromium benzenedicarboxylates. Eur J Inorg Chem. 2010;7:1043–8.
10. Devic T, Wagner V, Guillou N, Vimont A, Haouas M, Pascolini M, Serre C, Marrot J, Daturi M, Taulelle F, Férey G. Synthesis and characterization of a series of porous lanthanide tricarboxylates. Micropor Mesopor Mat. 2011;140:25–33.
11. Wang Z, Jin CM, Shao T, Li YZ, Zhang KL, Zhang HT, You XZ. Syntheses, structures, and luminescence properties of a new family of three-dimensional open-framework lanthanide coordination polymers. Inorg Chem Commun. 2002;5:642–8.
12. Soares-Santos PCR, Cunha-Silva L, Paz FAA, Ferreira RAS, Rocha J, Trindade T, Carlos LD, Nogueira HIS. Photoluminescent 3D lanthanide-organic frameworks with 2, 5-pyridinedicarboxylic and 1, 4-phenylenediacetic acids. Cryst Growth Des. 2008;8:2504–13.
13. Guo X, Zhu G, Li Z, Sun F, Yang Z, Qiu S. A lanthanide metal-organic framework with high thermal stability and available Lewis-acid metal sites. Chem Commun. 2006;30:3172–4.
14. Haitao X, Zhihua L. Microporous rare-earth coordination polymers constructed by 1, 4-cyclohexanedicarboxylate. Micropor Mesopor Mater. 2008;118:522–6.
15. Lama P, Aijaz A, Neogi S, Barbour LJ, Bharadwaj PK. Microporous La(III) metal-organic framework using a semirigid tricarboxylate ligand: synthesis, single-crystal to single-crystal sorption properties, and gas adsorption studies. Cryst Growth Des. 2010;10:3410–7.
16. Guo X, Zhu G, Li Z, Chen Y, Li X, Qiu S. Rare earth coordination polymers with zeolite topology constructed from 4-connected building units. Inorg Chem. 2006;45:4065–70.
17. Lin ZJ, Xu B, Liu TF, Cao MN, Lü J, Cao R. A series of lanthanide metal-organic frameworks based on biphenyl-3, 4, 5′-tricarboxylate; syntheses, structures, luminescence and magnetic properties. Eur J Inorg Chem. 2010;24:3842–9.
18. Black CA, Costa JS, Fu WT, Massera C, Roubeau O, Teat SJ, Aromi G, Gamez P, Reedijk J. 3-D lanthanide metal-organic frameworks: structure, photoluminescence, and magnetism. Inorg Chem. 2009;48:1062–9.
19. Gàndara F, de Andrés A, Gómez-Lor B, Gutiérrez-Puebla E, Iglesias M, Monge MA, Proserpio DM, Snejko N. A rare-earth MOF series; fascinating structure, efficient light emitters, and promising catalysts. Crys Growth Des. 2008;8:8378–80.
20. Binnemans K. Lanthanide-based luminescent hybrid materials. Chem Rev. 2009;109:4283–374.
21. Allendorf MD, Bauer CA, Bhakta RK, Houk RJT. Luminescent metal-organic frameworks. Chem Soc Rev. 2009;38:1330–52.
22. Eliseeva SV, Bünzli JCG. Lanthanide luminescence for functional materials and bio-sciences. Chem Soc Rev. 2010;39:189–227.
23. Qiong L, Huang RD, Xu YQ, Liu TF, Chu W, Hu CW. Syntheses, structures and properties of novel 3D lanthanide metal-organic frameworks with paddle–wheel building blocks. Inorg Chem Acta. 2008;361:2115–22.

24. Sarma D, Prabu M, Biju S, Reddy MLP, Natarajan S. Synthesis, structure and optical studies of a family of three-dimensional rare-earth aminoisophthalates. Eur J Inorg Chem. 2010;24: 3813–22.
25. Paz FAA, Klinowski J. Hydrothermal synthesis of a novel thermally stable three-dimensional ytterbium-organic frameworks. Chem Commun. 2003;103:1484–5.
26. Zheng X, Sun Ch, Lu S, Liao F, Gao S, Jin L. New porous lanthanide-organic frameworks: synthesis, characterization, and properties of lanthanide 2, 6-naphthalenedicarboxylates. Eur J Inorg Chem. 2004;16:3262–8.
27. Deng ZP, Huo LH, Wang HY, Gao S, Zhao H. A series of three-dimensional lanthanide metal-organic frameworks with biphenylethene-4, 4′-dicarboxylic acid: hydrothermal syntheses and structures. CrystEngCommun. 2010;12:1526–35.
28. Lin YW, Jian BR, Huang SC, Huang CH, Hsu KF. Synthesis and characterization of three ytterbium coordination polymers featuring various cationic species and a luminescence study o a terbium analogue with open channels. Inorg Chem. 2010;49: 2316–24.
29. Li XX, Wei ZQ, Yue ST, Wang N, Mo HH, Liu YL. A new lanthanide coordination polymer with 4, 4′-oxybis(benzoic acid) ligand: hydrothermal synthesis, crystal structure and photoluminescence. J Chem Crystallogr. 2011;41:757–61.
30. Wang YB, Sun CY, Zheng XJ, Gao S, Lu SZ, Jin LP. Synthesis and characterization of new polynuclear lanthanide coordination polymers with 4, 4′-oxybis(benzoic acid). Polyhedron. 2005;24: 823–30.
31. Liu GF, Qiao ZP, Wang HZ, Chen XM, Yang G. Synthesis, structures and photoluminescence of three terbium(III) dicarboxylate coordination polymers. New J Chem. 2002;26:791–5.
32. Wang Y, Wang Z, Yan C, Jin L. Hydrothermal synthesis and structure of new lanthanide coordination polymers with dicarboxylic acid and 1,10-phenantroline. J Mol Struct. 2004;692: 177–86.
33. Łyszczek R. Synthesis, structure, thermal and luminescence behaviors of lanthanide pyridine-3, 5-dicarboxylate frameworks series. Thermochim Acta. 2010;509:120–7.
34. Łyszczek R. Thermal investigations and infrared evolved gas analysis of light lanthanide (III) complexes with pyridine-3, 5-dicarboxylic acid. J Anal Appl Pyrolysis. 2009;86:239–44.
35. Łyszczek R, Iwan M. Investigation of desolvation process in lanthnthanide dinicotinates. J Therm Anal Calorim. 2011;103: 633–9.
36. Łyszczek R. Thermal and spectroscopic investigations of new lanthanide complexes with 1, 2, 4-benzenetricarboxylic acid. J Therm Anal Calorim. 2007;90:533–9.
37. Łyszczek R. Synthesis, characterization and thermal behaviour of hemimellitic acid complexes with lanthanides(III). J Therm Anal Calorim. 2008;91:595–9.
38. Trzaska-Durski Z, Trzaska-Durska H. Podstawy Krystalografii Strukturalnej i Rentgenowskiej. Warszawa: PWN; 1994.
39. Holly S, Sohar P. Absorption spectra in the infrared region. Budapest: Akadémiai Kiadó; 1975. p. 34–37, 108–109.
40. Silverstein RM, Webster FX. Spectrometric identification of organic compounds 6 st ed. 6th ed. New York: Wiley; 1996. p. 85–138.
41. Nunes RS, Bannach G, Luiz JM, Caires FJ, Carvalho CT, Ionashiro M. Thermal studies on solid 1,4-bis(3-carboxy-3-oxoprop-1-enyl)benzene of lighter trivalent lanthanides. J Therm Anal Calorim. doi:10.1007/s10973-010-1250-6.
42. Teixeira KC, Moreira GF, Quirino WG, Legnani C, Silva RA, Cremona M, Brito HF, Achete CA. Rare-earth based OLEDs. TG-FTIR thermal stability investigation of tetrakis beta-diketonates complexes. J Therm Anal Calorim. doi:10.1007/s10973-011-1564-z.
43. Bünzli JC. Lanthanide luminescence for biomedical analyses and imaging. Chem Rev. 2010;110:2729–55.